



An Investigation of the Ground Motion Scaling Procedures for the Nonlinear Seismic Analyses of Concrete Gravity Dams

Feyza Berat Soysal^a, Bekir Özer Ay^b, and Yalin Arici^a

^aDepartment of Civil Engineering, Middle East Technical University, Ankara, Turkey; ^bDepartment of Architecture, Middle East Technical University, Ankara, Turkey

ABSTRACT

Seismic assessment of gravity dams is generally carried out using time history analyses. Scaling of the motions is commonly used; however, in contrast to buildings, the performance of scaling procedures at predicting the mean and reducing the dispersion in engineering demand parameters (EDPs) is not known. The main goal of this study is to assess the performance of different scaling procedures in predicting seismic demands on dams. The performance regarding the prediction of the damage and the required number of motions for effective analysis was investigated. The results show that techniques commonly used for moment frames should not readily be applied to these structures.

ARTICLE HISTORY

Received 11 September 2016
Accepted 8 June 2017

KEYWORDS

Ground Motion Selection;
Ground Motion Scaling;
Nonlinear Analysis; Concrete
Gravity Dam; Damage Level

1. Introduction

The selection and scaling of accelerograms are some of the most important issues in earthquake engineering as ground motion records are widely being used in the design and evaluation of structures by engineers, replacing the response spectrum-based static analyses. The choice and the possible combinations of the ground motions add a significant layer of uncertainty to the prediction of the response of a structural system, which can hardly be addressed by trial and error methods even using today's powerful computers. As such, well-established and documented methods are necessary for the selection and scaling of accelerograms in order to better estimate the nonlinear structural response of a structure for an expected hazard by using real earthquake records.

A number of methods have been developed for the scaling of accelerograms for the nonlinear analysis of structural systems. The main objective of the use of scaling methods is to ascertain the accurate prediction of the response of a structure. The important question, however, is perhaps to define what an "accurate" prediction entails. Given that a set of time history analysis will always include a stochastic component compared with a response spectrum-based static analysis, an accurate analysis would mean: (1) capturing the expected performance level of the structure, parameterized in terms of the different engineering demand parameters (EDPs), (2) obtaining the aforementioned predictions with a level of certainty implying a limited variance in the analysis results, given the increase in the variance could mean questionable results, and (3) using a limited number of analyses and limited resources to reach the design or evaluation goal.

CONTACT Yalin Arici ✉ yarici@metu.edu.tr 📧 Department of Civil Engineering, Middle East Technical University, Ankara, 06800, Turkey.

© 2017 Taylor & Francis Group, LLC

The guidelines showing the appropriate ways of selecting and scaling suitable suites of accelerograms have not come to a desirable level yet [Bommer and Acevedo, 2004; Haselton, 2009] as the variability in the structural response due to the nature of input ground motions is unavoidable. In most design and evaluation methods, the analyst has to know the target of the analysis very well before choosing a method. Most of the selection methods can still not provide accurate estimates on the EDPs for some conditions and depend both on the nature of strong motion and on the site characteristics [Kalkan and Chopra, 2010]. It should also not be forgotten that the determination of the effectiveness of these ground motion scaling methods is a complicated issue because evaluations made by using numerical simulations may provide limited information and only a few studies have been performed with the experimental data [Kalkan and Chopra, 2011]. Consequently, seismic design codes provide limited guidance for the selection and scaling of earthquake ground motions. This situation yields to a range of problems in seismic design and may lead to misrepresentation of the seismic hazard situation by the voluntary or involuntary selection of input ground motions.

Concrete gravity dams are very important structures as their failure comprises a great risk to the society in terms of both life safety and economic consequences. The design and evaluation of these systems for seismic hazards are increasingly conducted using time history analyses given the need for the accurate prediction of the performance level of the existing dam inventory as well as the new systems. The primary structural damage on these systems is in the form of tensile cracking, which initiates on the downstream and upstream slopes of the monolith propagating toward the other side [Soysal et al., 2016]. The specific nature of loading is very important regarding the propagation of cracking on the unreinforced concrete [Tinawi et al., 2000]. Thus, for both evaluation and design, ground motion selection is a very important part of the process. The primary objective of this study, in this context, is to investigate the performance of different ground motion scaling procedures for the nonlinear time history analyses of concrete gravity monoliths with a focus on the accurate and effective prediction of the damage states on these systems. The performance of the scaling procedures was investigated for two different hazard levels obtained by conducting seismic hazard analyses for two separate dam sites. Sets of motions naturally matching these target levels were treated as benchmark sets in order to determine the target EDP levels. The performance of the scaling procedures, conducted using ground motion time histories (GMTHs) different from the benchmark set, was quantified in terms of their proximity to the design goals in terms of the mean values of the EDPs, along with considering the variances as indicators of the reliability and repeatability of the procedure.

This study is arranged as follows. A general discussion on the selection and scaling of the ground motion records is provided first in the next section, providing the necessary information on the scaling techniques, followed by the presentation of the two different sites considered in the study. The nonlinear modeling of concrete gravity dams and the validation studies undertaken to verify the use of modeling techniques for predicting the performance of plain concrete structures are presented in [Section 3](#) of this work. The performance of the chosen scaling procedures is evaluated in [Section 4](#) for different dam geometries by investigating the bias in the mean predictions as well as the amount of reduction in variance in the chosen EDPs. The necessary number of motions to be used for design purposes was investigated for each scaling

procedure in the final section. The conclusions of the study are presented in the final section.

2. The Selection and Scaling of the Ground Motion Records

For the design or evaluation of a structural system for seismic hazards, the earthquake records are recommended to be selected from the events whose magnitude, source-to-site distance, and type of faulting comply with the maximum earthquake considered at the site [USACE, 2003]. The use of a suite of GMTHs representing the physically realizable ground motion scenarios exercising the expected range of frequency content is recommended (USBR, 2013). The design documents recommend close cooperation with seismologists using site-specific hazard analyses for determining the suite of ground motions to be used in the transient analysis of dam systems: however, as mentioned before, there are no concrete suggestions regarding the selection method or the number of motions that should be used in a suite in contrast to the guidelines for similar analyses for moment frames. In order to evaluate the selection and scaling procedures in the context of dam systems, site-specific hazards from two different sites were considered in line with the general approach to the assessment of these systems. A ground motion database was formed in accordance with these hazard studies. The site-specific hazard analyses, the GMTH database, and the selected benchmark set of GMTHs are explained next, followed by a short description of the scaling procedures used.

2.1. Site-Specific Hazard Analysis and the Corresponding Target Response Spectra

The probabilistic seismic hazard analysis (PSHA) of two sites with different seismicity was conducted in order to consider alternative seismicity levels when interpreting the analysis results of this study. Located 45 km east of Erzurum city center, the first dam site was assumed on the Aras River in Eastern Anatolia. The site (site 1) is about 70 km away from the conjunction of the North Anatolian and Varto Faults, about 35 km away from the Erzurum fault zone and the Palandöken Fault, and about 10 km away from the Karayazi Fault. The second dam site (site 2) was assumed to be located near the eastern İstanbul suburban area. The distance between the dam site and the Marmara Sea segment of the North Anatolian Fault is about 36 km. Considering the soil characteristics at the first dam site, this study represents the site condition of both dams with a V_{S30} value of 760 m/s in PSHA calculations. The site conditions have an important influence on the ground motion records, particularly on their amplitude, frequency content, and duration [Kramer, 1996] and thus on the dam response. On the other hand, having a sufficient number of candidate records is a very important concern for obtaining unbiased results. Thus, in this study, the records having fairly similar ($520 \text{ m/s} < V_{S30} \leq 1070 \text{ m/s}$) site features [Ay and Akkar, 2012] with the dam sites were selected. Such an approach was inevitable especially for rock and hard rock sites, where the available number of records in strong ground motion databases is still very limited. Comparison of the spectral quantities for the selected records validates this approach: the records with relatively lower V_{S30} values compare fairly well with their counterparts as well as the target conditional spectrum within the period range of interest. The hazard levels of 475-year and 975-year return periods were used for sites 1 and 2, respectively. The de-aggregation of the hazard at the first site

yielded a moment magnitude (M_W) value of 5.6 and a source-to-site distance value of 12 km. The corresponding values were 7.1 and 35 km, respectively, for site 2. Using the hazard and corresponding de-aggregation information, conditional spectrum (CS) was derived for each site as the target to be used in the selection and scaling of ground motion records. The conditional mean spectrum (red solid line) and its variance (red dotted line) for the two dam sites described above are presented in Fig. 1.

2.2. The Ground Motion Database and the Selection of the Benchmark Set

The un-scaled records used in this study were gathered from the PEER NGA-West2 (<http://ngawest2.berkeley.edu>) ground motion database. Considering causal earthquake scenarios (magnitude and distance pairs) that had significant contribution to the exceedance of the ground motion intensity level, a candidate GMTH library was assembled for each dam site. For site 1, 319 records from 82 events were assembled in the candidate library. The M_W range covered by the candidate record library of site 1 was $5.0 \leq M_W \leq 7.0$, whereas the source-to-site distance (Joyner–Boore distance, R_{JB}) values extended up to 40 km. For site 2, $6.5 \leq M_W \leq 7.4$ and $5 \text{ km} \leq R_{JB} \leq 100 \text{ km}$ were used as the M_W and the source-to-site distance boundaries, respectively, which yielded 232 records from 21 events. For both sites, records having V_{S30} value less than 520 m/s, maximum usable frequency value larger than 1.65 Hz (considering twice the natural frequency, $2T^*$), and velocity pulses were excluded from the candidate library.

When selecting records for the dynamic analysis of structures, using each horizontal component individually or employing mutually perpendicular horizontal components as a unique candidate is usually decided with respect to the type of analysis and the response characteristics of the analyzed structure. Considering the dam response, the former approach in line with a recent study by Bernier *et al.* [2016] was used. Another issue related to the realistic simulation of dam response was taking the vertical component of

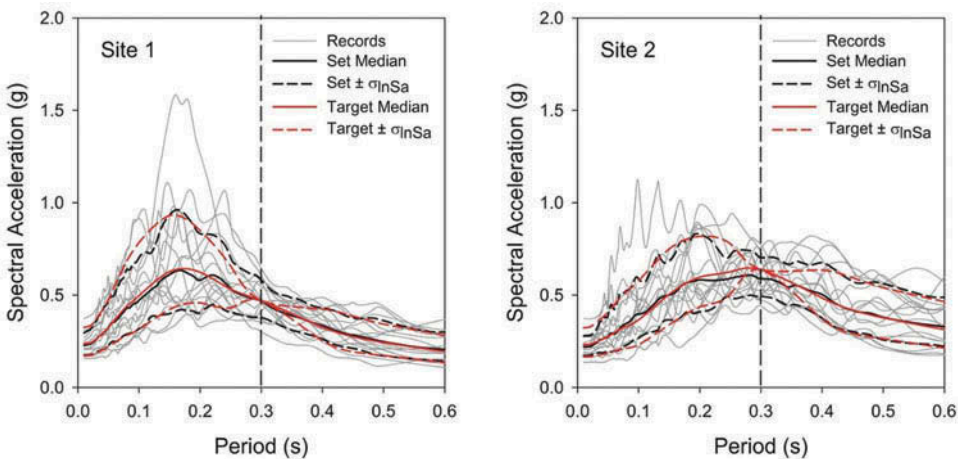


Figure 1. Acceleration spectra of the benchmark records, their mean, and variance compared with the target conditional spectrum.

ground motions into account [Bernier et al., 2016]. Thus, vertical components of the selected motions were also used in the dynamic analysis of the dams in this study.

The benchmark GMTH set for each site, which contained 15 un-scaled horizontal acceleration time-series, was obtained following the procedure proposed by Jayaram *et al.* [2011] and their vertical components were taken into consideration in the nonlinear analyses. The set that had the optimum match with the target mean and variance was determined as the one with the minimum sum of squared errors score [Jayaram et al., 2011] for a given period interval of $0.2T^*$ to $2.0T^*$, where T^* was the natural frequency of the monoliths. The relative weight of error in target mean with respect to error in target variance was taken as 50%. Among various numbers of records ranging from 7 to 30 in a set, the benchmark set with 15 records yielded a minimum SSE score, which was obviously case specific. Nevertheless, this simple yet objective measure is believed to yield unbiased results within the scope of this study. Besides these, further constraints were imposed for selecting the records among candidates. Maximum number of records from the same event was limited to one-third of the required number of records [Ay et al., 2017]. The spectra of the selected records (gray lines), their median (black solid line), and variance (black dotted line) are compared with the target CS in Fig. 1.

2.3. The Selection of the Comparison Set and the Scaling Procedures

To identify the records to be used in comparison of the scaling methodologies, the candidate bin used for the benchmark set was reduced in number. The records used for the benchmark analyses were removed from the library and new magnitude and distance bin limits were assigned. Mean magnitude ± 0.3 magnitude units and mean distance ± 25 km were used close to the values suggested by others [Stewart et al, 2001; Bommer and Acevedo, 2004; Ay and Akkar, 2012, etc.] as the limiting values. Instead of complete disaggregation information, which gives multiple causal earthquakes and their contribution to the hazard, the aforementioned limits on either side of the central values have been used in candidate selection in order to consider the usual practice where only the mean (or modal) values of magnitude and distance are available [Ay et al., 2017]. After scaling (as explained in Section 2.3.1) of the records in this constrained candidate set, the ground motion suite of 15 records was selected according to Jayaram *et al.* [2011]. When selecting the records, those having a scaling factor more than 5 (or less than 0.2) have been rejected by aiming both to limit the disproportionate modification and to have a fair amount of accelerograms that yield a reasonable match with the target. The same scaling factor was applied to both the horizontal and vertical components of each record in order to retain their genuine relation [Bommer and Acevedo, 2004]. The M_W , R_{JB} distance, and V_{S30} information of the selected records in the benchmark and comparison sets for sites 1 and 2 are presented in Table 1.

The effectiveness of nine different ground motion scaling procedures was investigated in this study:

- (1) Scaling to the acceleration value of the CS at conditioning period (SS)
- (2) Scaling to the acceleration spectrum intensity (ASI)
- (3) Scaling to the effective peak acceleration (EPA)
- (4) Scaling to the improved effective peak acceleration (IEPA)
- (5) Scaling to the peak ground acceleration (PGA) value

Table 1. M_W , R_{JB} , and V_{S30} for the benchmark and comparison sets selected for Sites 1 and 2.

Benchmark Set	M_W	R_{JB} (km)	V_{S30} (m/s)	Comparison Set	M_W	R_{JB} (km)	V_{S30} (m/s)
Site 1							
RSN707_H2	5.3	3.6	550	RSN45_H2	5.3	18.4	667
RSN769_H2	6.9	17.9	663	RSN414_H1	5.8	9.8	617
RSN809_H1	6.9	12.2	714	RSN501_H1	5.5	11.2	609
RSN954_H2	6.7	19.1	550	RSN1642_H1	5.6	17.8	680
RSN957_H2	6.7	15.9	582	RSN1642_H2	5.6	17.8	680
RSN1020_H1	6.7	20.8	602	RSN1649_H2	5.6	37.6	996
RSN1023_H2	6.7	24.9	671	RSN2385_H2	5.9	20.1	625
RSN1126_H1	6.4	14.1	650	RSN4278_H1	5.5	11.9	650
RSN1645_H2	5.6	2.6	680	RSN4278_H2	5.5	11.9	650
RSN2622_H1	6.2	15.0	625	RSN4312_H2	5.6	14.7	922
RSN4064_H2	6.0	4.3	657	RSN4369_H1	5.5	11.7	694
RSN4083_H1	6.0	4.7	907	RSN4509_H1	5.6	11.1	685
RSN4852_H1	6.8	30.3	606	RSN4509_H2	5.6	11.1	685
RSN4865_H1	6.8	5.0	562	RSN4513_H1	5.6	5.1	717
RSN5618_H2	6.9	16.3	826	RSN4513_H2	5.6	5.1	717
Site 2							
RSN80_H2	6.6	21.5	969	RSN291_H1	6.9	27.5	575
RSN587_H1	6.6	16.1	551	RSN810_H1	6.9	12.0	714
RSN989_H1	6.7	9.9	740	RSN1613_H2	7.1	25.8	782
RSN1058_H1	6.7	36.6	528	RSN1619_H1	7.1	34.3	535
RSN1618_H1	7.1	8.0	638	RSN1795_H1	7.1	50.4	686
RSN3943_H2	6.6	9.1	617	RSN1795_H2	7.1	50.4	686
RSN3954_H2	6.6	15.6	967	RSN4846_H1	6.8	28.1	606
RSN4455_H1	7.1	23.6	585	RSN4858_H1	6.8	25.4	640
RSN4843_H1	6.8	18.2	640	RSN4872_H2	6.8	21.2	640
RSN4852_H1	6.8	30.3	606	RSN4887_H2	6.8	36.6	562
RSN4865_H2	6.8	5.0	562	RSN5779_H1	6.9	36.3	540
RSN4870_H1	6.8	29.9	562	RSN5779_H2	6.9	36.3	540
RSN5478_H2	6.9	11.7	556	RSN5804_H1	6.9	25.6	562
RSN5618_H1	6.9	16.3	826	RSN5806_H1	6.9	22.4	655
RSN5809_H2	6.9	17.3	655	RSN6949_H1	7.0	52.1	551

- (6) Scaling to the geometric mean of maximum incremental velocity (MIV)
- (7) Scaling to the geometric mean of a pre-defined intensity measure (IM)
- (8) Scaling according to ASCE/SEI-7-10 specifications (ASCE)
- (9) Nonstationary spectral matching (RSPM)

A short summary of each procedure is given below.

2.3.1. Scaling to the Acceleration Value of CS at Conditioning Period (SS)

This scaling methodology modifies each record to equalize its spectral amplitude to the target value at the conditioning period (T^*). This technique, designated as stripe-scaling by Jalayer *et al.* [2007], is used widely as it is simple [Baker, 2011] and suitable for CS where the variance is zero at the conditioning period and nonzero at other periods [Jayaram *et al.*, 2011]. Since the natural frequencies of the monoliths were almost the same, 0.30 s was used in this study as the conditioning period ($T^* = 0.30$ s). The scale factor (SF) of each record was determined by Eq. (1). Target $S_a(T^*)$ values for sites 1 and 2 were 0.47 g and 0.64 g, respectively.

$$SF_{Record,i} = S_{a,target}(T^*)/S_{a,record,i}(T^*) \quad (1)$$

2.3.2. *Scaling to the ASI*

Scaling the ground motion records to the ASI measure was proposed by Von Thun *et al.* [1988]. ASI is defined as the area under the acceleration response spectrum for the period interval from 0.1 to 0.5 s. This parameter, well correlated with PGA and EPA [Yakut and Yılmaz, 2008], was deemed suitable for the structures sensitive to high-frequency motions such as concrete dams. In this study, target ASI level was determined from the CS for the given site and then each record in the comparison set was scaled such that their ASI values were equal to the target ASI.

2.3.3. *Scaling to the EPA*

EPA is the average of 5% damped acceleration response spectrum values between the periods of 0.1 and 0.5 s divided by 2.5 [ATC, 1978]. Similar to the ASI, it is well correlated with the PGA and suitable for structures having low to medium period values. In this scaling methodology, the EPA values of the records in the comparison set were linearly scaled to the target EPA value determined from the CS.

2.3.4. *Scaling to the IEPA*

IEPA is defined as 40% of the mean of the 5% damped spectral acceleration for the period interval given as $T \pm 0.2$ s. T is defined as the period where the maximum spectral acceleration occurs in order to take the different frequency contents of near-fault and far-fault ground motions into consideration [Yang *et al.*, 2009]. Yang *et al.* [2009] claimed that its correlation was better with the PGA and was preferable to EPA for near-fault motions.

2.3.5. *Scaling to the PGA*

PGA is a well-known and readily available parameter that is independent of the vibration characteristics of the structure to be analyzed. In this study, all records in the comparison set were scaled amplitude-wise to the target PGA, which was obtained as the mean PGA of the benchmark records for each site.

2.3.6. *Scaling for the Geometric Mean of MIV*

Incremental velocity is an IM for a ground motion defined as the area under the acceleration time history between two consecutive points of zero acceleration. The simplicity of application and the independence of the scaling factor from the natural frequency of the structure, which eliminates the effect of changes to the structural system on the scaling procedure, were suggested as the advantages of this scaling technique [Kurama and Farrow, 2003]. For the purpose of scaling of the records to the geometric mean of MIV, the procedure defined by O'Donnell *et al.* [O'Donnell *et al.*, 2013] was utilized. In this procedure, the ground motions are scaled to the geometric mean MIV of the benchmark suites, i.e. 0.18 and 0.24 m/s for the two target levels.

2.3.7. *Scaling for the Geometric Mean of a Damage IM*

Recently, a relationship was proposed in order to relate the ground motion parameters to the damage extent on dam monoliths [Soysal *et al.*, 2016]. The relationship, given in (2), was shown to provide a reasonable prediction on the damage level on a concrete monolith based on the PGA (cm/s^2) and the mean spectral velocity $S_{v,\text{mean}}$ ranging from $T_1(5\%)$ to

$1.3T_1(5\%)$ in cm/s. The proposed IM is dimensionless; the constants α and β were determined to be 0.0001 and 3, respectively [Soysal et al., 2016].

$$IM = \alpha [\log(S_{v,mean}) \times \log(PGA)]^\beta \quad (2)$$

The scaling of the ground motions to this IM was conducted in two steps. First, all motions were scaled to the benchmark geometric mean IM for the corresponding hazard level. Then, the spectrum of the geometric mean of the scaled motions was compared to the target spectrum. If the mean spectrum was below the target spectrum, another SF was defined to match the target earthquake spectrum. Given the almost identical natural frequencies of the chosen monoliths, the same SFs were used for all the models.

2.3.8. ASCE/SEI-7-10-Based Time History Scaling

For the scaling of more than seven records, ASCE/SEI-7-10 [ASCE, 2010] requires intensity-based scaling using appropriate SFs so that the mean value of the 5%-damped response spectra for the set of scaled records is not less than the design response spectrum over the $0.2T_1$ – $1.5T_1$ period range. As the procedure for scaling is not explicitly provided in ASCE/SEI-7-10, the procedure defined in Kalkan and Chopra [2010] was used in this study. This procedure suggests obtaining a scale factor (SF_1) for each of the motions through a least square fit method. After each motion is scaled for these factors, the geometric mean of spectra is calculated. According to ASCE/SEI-7-10, the mean spectrum should not be less than the target spectrum between periods of $0.2T_1$ and $1.5T_1$. To address this issue, the minimum of the spectrum is compared to the target spectrum once more and a new scale factor (SF_2) is defined to cover the maximum difference between the average and target spectra (ϵ_{asce}).

2.3.9. RSPM

For the purpose of conducting RSPM of ground motion records, the well-known SeismoMatch software [Seismosoft, 2013] that utilizes the algorithm proposed by Hancock et al. [2006] was used in accordance with the guidelines provided in USACE-EM 1110-2-6051 [USACE, 2003]. After each matching, the authenticity of the ground motion developed was checked in order not to have any unrealistic pulse or duration content within the ground motion. The final spectra were compared to the target spectrum.

The scaling factors for a given record and scaling methodology (except spectral matched records) are presented in Table 2 for site 1 (upper panel) and site 2 (lower panel). In this study, the scaling factors were applied to both the horizontal and vertical components of each record as discussed in Section 2.3.

3. Nonlinear Transient Analysis of Concrete Gravity Dams

3.1. Analysis Models

The general-purpose finite element software, DIANA [DIANA, 2014], was used as the computational platform to simulate the dam–reservoir–foundation system behavior [DIANA, 2014] in this study. DIANA allows the nonlinear transient analysis of 2D and 3D systems with higher-order elements using the implicit integration technique. The software allows the use of fluid elements for the reservoir and absorbing boundaries for

Table 2. Scaling factors for different scaling methodologies, comparison sets, Site 1 (upper panel), and Site 2 (lower panel).

	SS	ASI	EPA	IEPA	PGA	MIV	IM	ASCE 7-10
Site 1 records								
RSN45_H2	1.86	1.38	1.61	1.35	1.46	1.93	1.61	1.91
RSN414_H1	2.53	1.88	2.04	1.89	1.91	2.15	2.17	2.18
RSN501_H1	4.79	5.33	5.41	5.62	5.45	4.99	2.01	5.63
RSN1642_H1	0.57	0.72	0.75	0.74	0.79	0.72	0.82	0.77
RSN1642_H2	1.49	1.17	1.19	1.01	0.90	1.10	1.17	1.17
RSN1649_H2	4.18	3.50	3.89	3.26	1.89	3.44	4.66	4.11
RSN2385_H2	1.82	1.89	1.89	1.97	2.36	1.83	1.65	1.97
RSN4278_H1	3.56	2.71	2.85	2.65	2.64	2.72	3.02	2.91
RSN4278_H2	1.68	2.08	2.15	2.23	2.63	1.96	2.66	2.22
RSN4312_H2	3.04	2.79	2.91	2.89	3.52	2.80	2.80	3.03
RSN4369_H1	1.48	1.75	1.79	1.76	1.45	1.71	1.71	1.87
RSN4509_H1	1.05	1.62	1.64	1.65	1.62	1.38	1.43	1.76
RSN4509_H2	2.03	1.70	1.78	1.77	2.23	1.93	1.73	1.88
RSN4513_H1	3.38	3.19	3.25	3.32	2.61	3.23	1.52	3.43
RSN4513_H2	2.26	2.57	2.56	2.64	2.86	2.60	2.13	2.59
Site 2 records								
RSN291_H1	2.44	2.01	1.97	2.56	2.42	2.38	2.27	2.21
RSN810_H1	0.59	0.45	0.43	0.56	0.51	0.88	0.43	0.51
RSN1613_H2	4.41	3.83	3.82	4.97	4.38	5.19	4.24	4.50
RSN1619_H1	1.09	1.73	1.75	1.75	1.93	2.05	1.36	2.00
RSN1795_H1	4.17	3.18	3.20	3.48	3.01	2.20	3.27	3.57
RSN1795_H2	2.22	2.41	2.45	2.77	2.65	3.56	2.59	2.86
RSN4846_H1	0.58	0.67	0.65	0.60	0.71	0.54	0.53	0.74
RSN4858_H1	0.99	1.02	0.97	0.90	1.12	1.11	0.83	1.02
RSN4872_H2	2.00	1.83	1.81	2.27	1.87	1.13	1.76	2.04
RSN4887_H2	1.68	1.72	1.65	1.46	1.90	1.12	1.38	1.88
RSN5779_H1	2.94	3.06	2.96	3.05	3.23	1.13	2.82	3.34
RSN5779_H2	1.52	1.50	1.49	1.56	1.44	0.96	1.32	1.68
RSN5804_H1	1.04	0.91	0.90	0.93	0.80	1.01	0.82	0.95
RSN5806_H1	1.20	1.12	1.09	1.46	0.98	0.69	1.00	1.24
RSN6949_H1	1.70	1.85	1.80	1.80	1.91	1.49	1.75	2.06

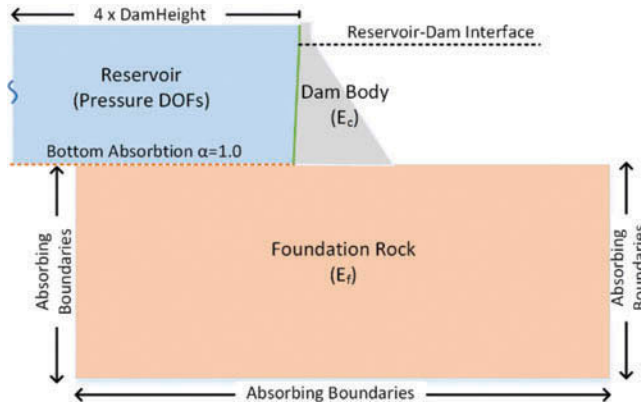


Figure 2. Analytical model for the dam–reservoir–foundation system.

the foundation media required for the accurate simulation of the dam response (Fig. 2). The dam body (a 20-m-wide monolith, $E_c=31$ GPa) was modeled using second-order plane-stress elements with four integration points, while the foundation ($E_f = 61$ GPa) was modeled using triangular plane-stress elements with three integration points.

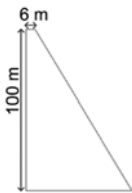
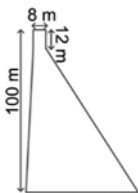
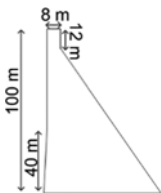
The reservoir–dam interaction was modeled using flow elements with pressure degrees of freedom incorporating fluid–structure interaction elements coupling the pressure and displacement degrees of freedom at the interface between the reservoir and the upstream face of the dam. For all of the models, the reservoir ($\rho = 1000 \text{ kg/m}^3$) height was assumed as 98 m and the reservoir was modeled using compressible fluid elements with pressure degrees of freedom and absorbing elements on the outgoing end (Fig. 2) located at 400 m from the upstream of the monolith. The sonic speed was assumed at 1438 m/s for the reservoir medium. The bottom absorption coefficient for the reservoir was assumed as 1.0 assuming a design scenario for the system. Absorbing boundary conditions [Lysmer and Kuhlemeyer, 1969] were used at the bottom and the sides of the foundation along with a typical hysteretic damping of 10% [USBR, 2013; Bernier et al., 2016]. A complete list of material properties is presented in Table 3. The model was validated by comparing the frequency response to the results from the EAGD84 software [Fenves and Chopra, 1984] with 1.5% and 5% damping for the dam body and foundation, respectively. The transfer function for the crest acceleration at the crest was compared to the frequency domain counterpart validating the modeling parameters. Stiffness proportional Rayleigh damping coefficients were used in the model, obtaining frequency response of the monoliths in reasonable agreement with the exact frequency domain solution.

The analyses in this study were conducted for three different 100-m-tall monoliths (Table 4) in order to incorporate the possible effect of the geometry into the investigation. The first of these cross-sections was based on the design of a dam system in Turkey, while the other geometries were selected from typical dam geometries given in Chopra and Chakrabarti [1973]. The geometry of each cross-section was defined in order to obtain similar cross-sectional areas. The upstream face of the first monolith was assumed vertical, while the downstream side had a slope of 1H/0.6V. The upstream and downstream slopes

Table 3. Material properties assigned to the models.

Material property	Structure	Foundation
Young's modulus (GPa)	31 GPa	62 GPa
Poisson's ratio	0.2	0.3
Density (kg/m^3)	2400	2500
Stiffness proportional damping coefficient	0.00125	0.008

Table 4. Geometric properties of the structural models.

			
	Model 1	Model 2	Model 3
Height(m)	100	100	100
U/S Slope	Vertical	1V/0.05H	1V/0.05H
D/S Slope	1V/0.6H	1V/0.65H	1V/0.7H
$T_n(\text{sec})$	0.32	0.30	0.31

of the second monolith were 0.05V/1H and 1H/0.65V, respectively, introducing discontinuity points at the “neck” of the structure. Similarly, the upstream and downstream slopes of the third monolith were 0.05V/1H and 1H/0.7V, respectively. However, for this monolith, the discontinuity at the upstream face is located at a lower elevation of 40 m. The element sizes for the dam body were set at around 0.9 m for all models corresponding to approximately 6000 elements and 28000 degrees of freedom on the dam body.

For the nonlinear transient analyses, a constant time increment of 0.005 s was used with the Newmark average acceleration time-stepping algorithm. Both the lateral and vertical components of the ground motion were applied to the models simultaneously. The cracking in the dam was modeled using the robust smeared cracking formulation [Rots et al., 1988; Yamaguchi et al., 2004] widely utilized in the literature for the prediction and evaluation of the performance of monolithic concrete structures. A fracture energy of 140 N/m was used in accordance with the tensile strength of the concrete, which was assumed as 1.95 MPa for this case. The compressive strength of concrete was assumed as 20 MPa. The exponential and parabolic functional forms of softening were used for the tensile and compressive unloading branches, respectively. The summary of two different validation studies, conducted to verify the use of the smeared crack model in transient analyses, is presented below.

3.2. Smeared Crack Model for Crack Propagation in Concrete and the Validation Studies

The smeared cracking approach is regarded as a well-established constitutive model for determining the seismic behavior of plain concrete structures using continuum models. The uncracked concrete behaves in an elastic isotropic fashion; after the occurrence of cracking, the stress is determined in the direction given by the cracking and the stress-strain laws in tension and compression are employed in the rotated coordinate system. The tensile (f_t) and compressive strengths (f_c) and the shape of the post-peak response are the key characteristics of the stress-strain models. The mesh dependence of such models was addressed using the fracture energy (G_f). Secant unloading is applied during cyclic loading [Rots, 1988]. The smeared crack models were used extensively for predicting the performance of the Koyna and Pine Flat Dams [Bhattacharjee and Leger, 1994; Ghaemian and Ghobarah, 1999; Mirzabozorg and Ghaemian, 2005; Çalayır and Karaton, 2005; Hariri-Ardebili, 2014; Hariri-Ardebili et al., 2016]. The smeared crack model used in this study was validated using two well-documented laboratory tests as given below.

3.2.1. Pseudo-Dynamic Testing of a Scaled RCC Dam Monolith

A 1/75 scaled model of the 120-m-high Melen Dam was tested by Aldemir *et al.* [2015] using three different scaled ground motions in a pseudo-dynamic setup (Fig. 3). The special setup of the test enabled the use of only the bottom half of the dam section; the inertial and hydrodynamic load effects were simulated using a special loading apparatus. The hydrodynamic loads were included in the test set by determining an optimal equivalent mass on the system, yielding a similar overturning moment-base shear response with respect to the rigorous solution of the system with the software EAGD [Fenves and Chopra, 1984]. Equivalent mass values were determined for the three earthquake levels,

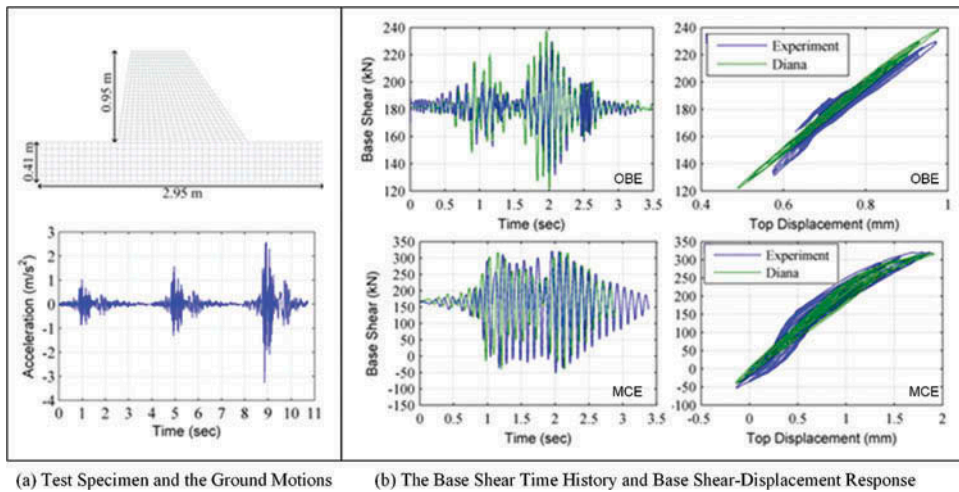


Figure 3. Pseudo-dynamic test on the scaled model of the Melen dam, experiment versus the simulation results.

namely the Operational Based Earthquake (OBE), the Maximum Design Earthquake (MDE), and the Maximum Characteristic Earthquake (MCE) levels. These mass values, incorporated in the pseudo-dynamic testing algorithm, enabled the determination of the time-varying lateral force on the test specimen. The corresponding force, as applied to the test specimen, was directly used as the applied force in the validation study.

The finite element used in the validation study consisted of 764 second-order elements. The flexibility at the base of the specimen was taken into account by using spring elements at the base to match the natural frequency of the uncracked state of the specimen. The tensile strength, modulus of elasticity, and the subgrade modulus used were 1.0 MPa, 15 GPa, and 385 MPa, respectively, while the fracture energy was assumed as 40 N/m. The geometry of the specimen, the utilized ground motions, and the corresponding spectra at the OBE, MDE, and MCE levels are presented in Fig. 3a. Consecutive nonlinear transient analysis was conducted with linear softening for the model along with the above-mentioned properties for the material. The time histories for the base shear and the base shear–crest displacement relationships for the OBE and MCE levels are presented in Fig. 3b. The capacity of the system was predicted well for the MCE level although the base shear was overestimated for the OBE level. The failure to perfectly capture the limited cracking on the system during the hydrostatic loading, possibly due to a casting issue, led to an overprediction of the base shear for the OBE case; however, for the high-damage MCE scenario, the capacity was estimated well.

3.2.2. Shake Table Testing of a Concrete Monolith

The experimental results of Tinawi *et al.* [Tinawi *et al.*, 2000] were reproduced in order to determine the efficiency of the analytical predictions for the behavior of concrete gravity dams. In this experiment, a plain concrete gravity dam specimen having a height of 3.4 m was tested using a pulse excitation (Fig. 4) at three different intensity levels. The pulse was scaled with respect to its first peak acceleration (FPA) to three levels: 0.87, 0.94, and 0.98 g. The tests with the FPA of 0.94 g and 0.98 were referred to as the first and second cracking

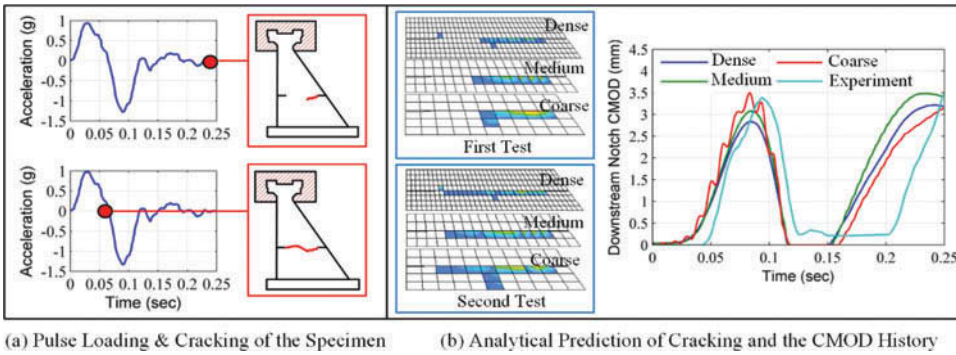


Figure 4. Shake table test on a scaled dam model (Tinawi et al., 2000), experiment vs. the simulation results.

tests, respectively [Tinawi et al., 2000], as the first test with the FPA of 0.87 did not lead to any cracking on the specimen. The well-documented experiment provided an excellent opportunity to calibrate the material models. Along with the displacement time histories, the cracking pattern and timing were sought to be represented in the analytical model. The results of the validation study (Fig. 4b) show that the crack propagation on the monolith was captured well with models using different element sizes with little sensitivity to the mesh density used. The crack opening at the notch was predicted satisfactorily as well using the smeared crack model for nonlinear analysis.

3.3. The Benchmark Solution and the Selected EDPs

The EDPs for the concrete gravity dams are not as well established as the corresponding parameters commonly used for the moment frame structures such as the inter-story drift ratios. The crest displacement and acceleration are often reported in a design process given these can be measured easily in the existing structures with the help of seismic instrumentation. However, the verification of the association of these parameters with the damage levels on these systems is scarce [Alembagheri and Ghaemian, 2012; Soysal et al., 2016]. Given the analyses conducted allow a range of performance parameters to be obtained from the models, the crest displacement, accelerations, and the ratio of the area of the damaged elements to the total area of the monolith were selected as the demand parameters of interest in this study. The cracked area ratio [Çalayır and Karaton, 2005], defining the amount of cumulative damage on a dam monolith, was determined to be reasonably correlated to the damage state on a dam, which could be used for decision-making purposes [Soysal et al., 2016]. Sample cracking patterns for model 1 (Table 4) are presented in Fig. 5 in order to demonstrate three different damage states on the system, corresponding to different cracked area percentages. The detailed explanation of the damage states and the relation to EDPs can be found in Soysal et al. [2016].

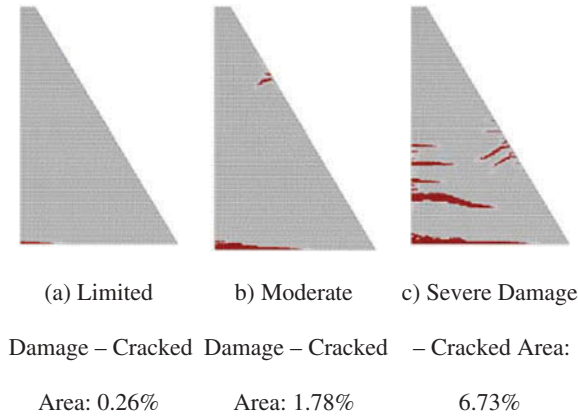


Figure 5. Sample cracking schemes for the limited, moderate, and severe damage cases.

4. Analysis Results

Approximately 1000 nonlinear transient analyses were performed for the three different dam monoliths in order to evaluate the GMTH scaling procedures. The first set of analyses was conducted with the benchmark sets (un-scaled) for the two selected sites. Then, the analyses with the comparison sets were conducted using nine scaling techniques introduced in Section 2. The EDPs, i.e. the maximum crest acceleration, displacement, and the ratio of the cracked area of the given monolith to the total area of the system, were obtained for each model. The results from the sets were compared to the benchmark results using the median values and the dispersion measures. The median value \bar{x} and the corresponding dispersion measure δ for EDPs for each set were calculated as follows [Kalkan and Chopra, 2011]:

$$\bar{x} = \exp\left(\frac{\sum_{i=1}^n \ln x_i}{n}\right) \quad \delta = \exp\left(\frac{\sum_{i=1}^n (\ln x_i - \ln \bar{x})^2}{n-1}\right)^{1/2} \quad (3)$$

where x_i is the value of the EDPs and n is the number of observations (15 for this study). Considering the important effect of loading direction, the benchmark results were obtained as given in the next section.

4.1. Benchmark Results Considering the Effect of Direction

In contrast to many of the moment frame structures, the dam monoliths are not built with symmetric cross-sections, i.e. one side of the cross-section is already under significant distress due to the hydrostatic forces. Given the asymmetrical resistance of the section for loading in the downstream (D/S) and the upstream (U/S) direction [Soysal et al., 2016], for obtaining the benchmark results, the effect of ground motion direction on the response was considered. The un-scaled motions were first applied on the dam from the upstream direction to the downstream direction. The same un-scaled motions were then applied from the downstream direction to the upstream direction of the dam. The mean and standard deviation values for the chosen EDPs obtained henceforth are shown in Table 5;

Table 5. The mean and dispersion for the EDPs from un-scaled ground motions (benchmark sets).

	Max. Acc.(m/s ²)		Norm. Max. Disp. (%)		Cracked Area (%)	
	\bar{x}	δ	\bar{x}	δ	\bar{x}	δ
(a) Target Spectrum I						
Model 1 (+)	22.40	1.39	0.038	1.17	0.85	2.18
Model 1 (-)	22.28	1.37	0.041	1.08	0.94	1.77
Model 2 (+)	27.12	1.30	0.046	1.16	1.10	2.56
Model 2 (-)	27.85	1.31	0.048	1.18	1.38	2.02
Model 3 (+)	27.81	1.29	0.046	1.16	1.14	2.54
Model 3 (-)	27.56	1.28	0.048	1.18	1.45	2.12
(b) Target Spectrum II						
Model 1 (+)	18.89	1.37	0.047	1.16	2.22	2.13
Model 1 (-)	19.34	1.34	0.049	1.23	2.76	2.14
Model 2 (+)	24.39	1.32	0.054	1.18	2.55	2.14
Model 2 (-)	25.30	1.32	0.057	1.27	2.95	2.39
Model 3 (+)	25.22	1.36	0.054	1.17	2.88	2.04
Model 3 (-)	26.12	1.35	0.058	1.27	3.41	2.43

results in the negative direction are indicated with the symbol (-). Comparison of the mean (\bar{x}) values of the EDPs for the motions applied in the opposite directions shows that the effect of ground motion direction was not very significant for the acceleration and displacement EDPs. However, there were significant differences among the cracked area ratio for the two sets. For example, the crack area ratio for the negative direction of the motion was around 20% larger compared with the positive direction for the target spectrum II.

Such a difference among the results of the EDPs prompted further investigation on the effect of direction to quantify the statistical effect of the direction on EDPs. There was a large combination of sets that could be formed considering the positive or negative direction of the motions given the direction effect is generally not included within the design process or during the seismic hazard study. The statistics of the EDPs for the 2¹⁵ sets that can be formed out of the selected 15 motions was compiled. In order to demonstrate the effect of direction on the analysis results, the normalized histograms of the EDPs for model 2 are presented in Fig. 6, representing the results from all sets with possible variations in direction included. To quantify the variation in the data, some statistical limits were also drawn on the chart: the red line in the figures shows the mean of these estimates, while the blue lines provide the $\pm 5\%$ bounds on the mean. The results shown in Fig. 6 indicate that the direction effect was not significant on the displacements (as well as accelerations not shown for brevity). However, the direction affected the cracked area estimate much more severely: the chosen benchmark level lied near the median EDP level for Target I, while it was approximately 10% off the median level for Target II considering the direction effect.

4.2. Statistical Investigation of the Scaling Techniques' Effectiveness

A total of 810 different time history analyses were conducted for the three different gravity dam models at two hazard levels. Nine different ground motion suites each consisting of 15 different GMTHs were used for this purpose. The considerable output obtained from these analyses was summarized in terms of the aforementioned EDPs for comparison purposes. As mentioned above, the results from the analyses with the un-scaled ground motions (in + direction) are denoted as "benchmark" in the next section, while the acronyms for the scaling

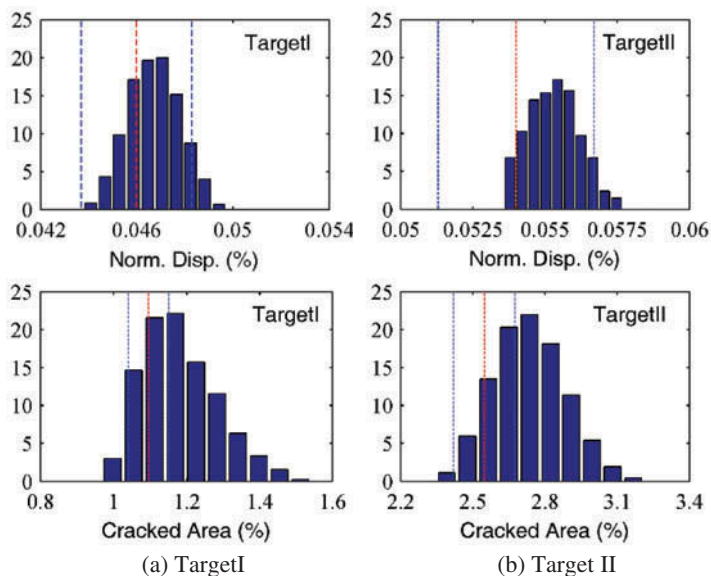


Figure 6. Normalized histogram of the EDPs, considering the direction effect on the whole suit for Model 2, benchmark positive $\pm 5\%$ bounds shown.

methods “SS”, “ASI”, “EPA”, “IEPA”, “PGA”, “MIV”, “IM”, “ASCE”, and “RSPM” were used as the shorthand notations while presenting the results for the individual scaling techniques presented in Section 2. EDPs were chosen as the commonly used indices for the performance of the structure. As a simple mean to assess the performance level of a monolith, the ratio of the cracked area to the total cross-sectional areas of the dams was used. To simplify the interpretation, the displacements were normalized by dam height.

The comparison of the results was made by comparing the geometric mean and the dispersion measure of the EDPs obtained for each scaling procedure to the benchmark result for each model. For each set of dynamic analyses, the mean of the maximum acceleration, displacement, and the cracked area ratio were calculated and compared with the corresponding benchmark value and the results obtained from the other sets of analyses. The mean value of the results obtained from each scaled motion set should be in line with the mean value of the un-scaled benchmark. The dispersion in the results should be reduced by the scaling procedure. Arguably, the accurate prediction of the mean EDP quantity is more important in showing the performance of the procedure; however, it should not be forgotten that an accurate mean prediction with a large dispersion would imply that a significant number of ground motions will have to be included in a given set in order to ascertain the consistency among possible motion sets.

The mean and dispersion values of the crest acceleration obtained from the suites scaled with different procedures are presented in Table 6. The results are presented separately for the different monoliths and target spectra. The benchmark values are reported directly in the table. The relative differences of the mean and the dispersion value from the benchmark quantity calculated as $\varepsilon_{EDP} = (x_{scaled} - x_{bm})/x_{bm}$ were calculated for directly assessing the performance of the scaling procedure. It should be noted that when the percent relative difference was a positive value, the results of the scaled sets

Table 6. The mean and dispersion for the crest acceleration (m/s^2) EDP for different scaling procedures.

	Mean values (\bar{x})						Dispersion values (δ)					
	Target spectrum I			Target spectrum II			Target spectrum I			Target spectrum II		
	M1	M2	M3	M1	M2	M3	M1	M2	M3	M1	M2	M3
Bench.	15.657	16.823	17.788	15.115	17.105	17.479	2.009	1.751	1.742	2.011	1.757	1.741
% Relative difference from benchmark, mean, and dispersion measure												
SS	2.7	14.1	9.0	6.2	4.8	3.3	0.8	5.1	6.4	-4.5	-2.7	-5.5
ASI	-2.0	10.1	10.2	4.1	3.3	-2.1	-13.4	-5.4	-6.7	-12.4	-8.4	-13.3
EPA	2.1	13.9	14.5	3.0	1.7	-2.5	-10.7	-3.6	-5.7	-12.3	-7.9	-10.6
IEPA	-1.2	11.9	11.1	10.6	10.4	7.6	-15.4	-7.2	-10.0	-10.4	-2.1	-4.8
PGA	-1.7	8.0	5.3	8.4	8.4	4.7	-12.2	-5.4	-7.7	-12.9	-5.0	-9.7
MIV	-8.6	0.2	0.2	-3.7	-3.2	-8.1	7.9	13.8	13.4	6.4	13.0	7.0
IM	1.3	9.6	7.8	-1.1	-2.2	6.3	-6.3	-2.3	-2.7	-11.0	-6.1	-11.3
ASCE	6.9	20.2	17.1	13.1	10.8	6.3	-7.9	-3.7	-6.4	-13.9	-5.6	-11.3
RSPM	-6.5	3.8	0.0	-2.3	-2.3	-3.3	-20.8	-9.6	-9.5	-12.7	-10.0	-12.6

were higher and when it was negative, the results were lower than the benchmark value. For instance, for model 1, the mean crest acceleration for the suite scaled with the RSPM method was 6.5% less than the benchmark estimate. The dispersion was reduced by 20.8% from the benchmark using the scaling technique.

The mean values of the crest acceleration EDPs from the scaled ground motions are within +20 to -10% of the benchmark results. In general, the mean EDP was predicted to be higher compared with the benchmark analyses (Table 6). The results from the ASCE and IEPA scaling were considerably higher than the benchmark results for both target levels. On the other hand, the RSPM, PGA, and ASI scaling yielded close estimates for the benchmark results. For some of the scaling methods (EPA, IEPA, and ASI), the results for the scaled sets were markedly different at the two hazard levels: the overestimation of the benchmark mean was reduced for the second target spectrum. The reduction in the dispersion was utmost 20% for the scaling methods. The most significant reduction was obtained using RSPM, EPA, and ASI scaling. Compared with models 2 and 3, the dispersion in the estimate was reduced more for model 1. Overall, the reduction in the dispersion was similar for both target spectra.

Table 7. The mean and dispersion for the normalized crest displacement ($\Delta_{crest}/H(\%)$) EDP for the different scaling procedures.

	Mean values (\bar{x})						Dispersion values (δ)					
	Target spectrum I			Target spectrum II			Target spectrum I			Target spectrum II		
	M1	M2	M3	M1	M2	M3	M1	M2	M3	M1	M2	M3
Bench.	0.032	0.036	0.036	0.031	0.034	0.034	1.723	1.735	1.741	1.670	1.684	1.695
% Relative difference from benchmark, mean, and dispersion measure												
SSS	8.6	11.7	13.0	-12.4	4.8	5.9	0.1	5.6	6.1	-0.7	0.9	2.2
ASI	6.0	9.1	11.0	13.2	4.7	4.0	-1.9	-1.7	3.1	0.6	0.6	1.2
EPA	9.5	13.6	16.0	-14.1	2.9	2.3	-2.7	2.5	2.8	-0.7	0.4	0.7
IEPA	6.7	10.6	13.1	-7.6	9.7	10.8	1.1	4.6	5.0	-2.1	3.1	4.1
PGA	7.0	11.7	12.3	-10.7	8.6	8.5	10.6	17.5	17.8	1.8	3.6	4.1
MIV	1.8	3.4	4.3	-19.5	-6.5	-6.9	9.4	20.3	20.2	13.8	19.0	17.4
IM	7.6	10.0	11.7	-17.1	-1.8	14.0	-2.2	2.6	3.5	-4.1	-2.1	2.5
ASCE	13.6	19.5	21.6	-6.7	13.0	14.0	-2.0	3.8	3.7	-1.0	0.9	2.5
RSPM	3.9	9.0	11.1	-11.9	3.0	2.9	-5.5	-5.0	-4.9	-5.4	-4.6	-4.4

The mean and dispersion values of the normalized crest displacement obtained from the ground motion suite scaled with different procedures are presented in Table 7. The normalized crest displacement was generally predicted higher by the scaled sets compared with the un-scaled benchmarks values. The results were within 5–20% of the benchmark displacement values. The ASCE, EPA, and IEPA scaling yielded the highest estimates. The dispersion for the scaled sets was generally similar to the benchmark set, with perhaps the only meaningful reduction obtained with the spectral matching technique. There did not appear to be a major difference for dispersion reduction with respect to the target spectrum.

The mean and dispersion values of the total cracked area on the monolith obtained from the ground motion suite scaled with the different procedures are presented in Table 8. The presented quantities were normalized by the total cross-sectional area of the concrete gravity dam in order to obtain the percentage of the cracked area on the monolith. The results obtained from the scaled suites were generally larger than their counterparts obtained from the original ground motion suite. Notably, the ASCE scaling yielded significantly higher damage area ratios (as much as 100% over the benchmark) compared with the other scaling techniques. The IEPA yielded high predictions as well for the first spectrum. The MIV and RSPM scaling on the other hand yielded predictions on the downside of the benchmark. The mean crack area ratio predicted from the RSPM scaling was as much as 30% lower than the benchmark value. The reduction of dispersion varied significantly for the two different target spectra. The reduction was markedly higher for the second spectrum, varying between 15 and 25%, with the RSPM scaling reducing the dispersion by as much as 38% for the first model. The reduction in dispersion was smaller for the first target spectrum: for some models, the dispersion was even increased compared with the benchmark set after the scaling.

The overall comparison of the scaling procedures is presented in Fig. 7 for the chosen EDPs. For each model, the mean prediction from the scaled set along with \pm standard deviation on the predictions can be seen on the figure. The mean estimates for the crest acceleration and displacement were quite close to the benchmark results. The results were mixed regarding the estimation of the cracked area ratios. The dispersion in this quantity was substantial compared with the previous EDPs. The reduction in the dispersion for the scaled sets was observed consistently for the crest acceleration EDP: for the other EDPs, an

Table 8. The mean and dispersion for the total cracked area ratio EDP for the different scaling procedures.

	Mean values (\bar{x})						Dispersion values (δ)					
	Target spectrum I			Target spectrum II			Target spectrum I			Target spectrum II		
	M1	M2	M3	M1	M2	M3	M1	M2	M3	M1	M2	M3
Bench.	0.849	1.096	1.142	2.216	2.548	2.876	2.180	2.557	2.537	2.130	2.140	2.040
% Relative difference from benchmark, mean, and dispersion measure												
SS	5.2	36.4	45.9	-8.6	13.5	17.2	4.9	0.9	14.0	-22.8	-17.5	-15.5
ASI	-9.0	8.6	18.2	-10.4	8.1	5.8	7.6	-15.1	-5.1	-16.2	-15.7	-16.2
EPA	1.3	35.1	52.5	-14.8	-0.3	1.4	-4.9	-11.4	0.1	-16.3	-18.4	-16.0
IEPA	-7.9	2.2	24.8	11.3	36.9	36.8	11.7	-0.9	2.8	-21.7	-21.7	-20.2
PGA	-5.8	22.6	28.2	1.8	31.6	30.4	57.1	49.2	71.0	-3.8	-13.4	-18.5
MIV	-24.4	-8.3	-9.0	-32.1	-32.6	-38.5	26.8	61.6	89.5	64.8	71.6	74.3
IM	-9.5	27.4	40.2	-27.1	-17.9	49.2	-9.2	-3.4	3.3	-30.5	-30.7	-24.1
ASCE	14.2	69.7	107.3	16.7	51.7	49.2	-8.7	-7.2	3.2	-17.7	-23.4	-24.1
RSPM	-17.4	-34.1	-27.2	-4.5	-3.8	2.4	-34.5	-30.9	-23.0	-37.8	-28.5	-27.0

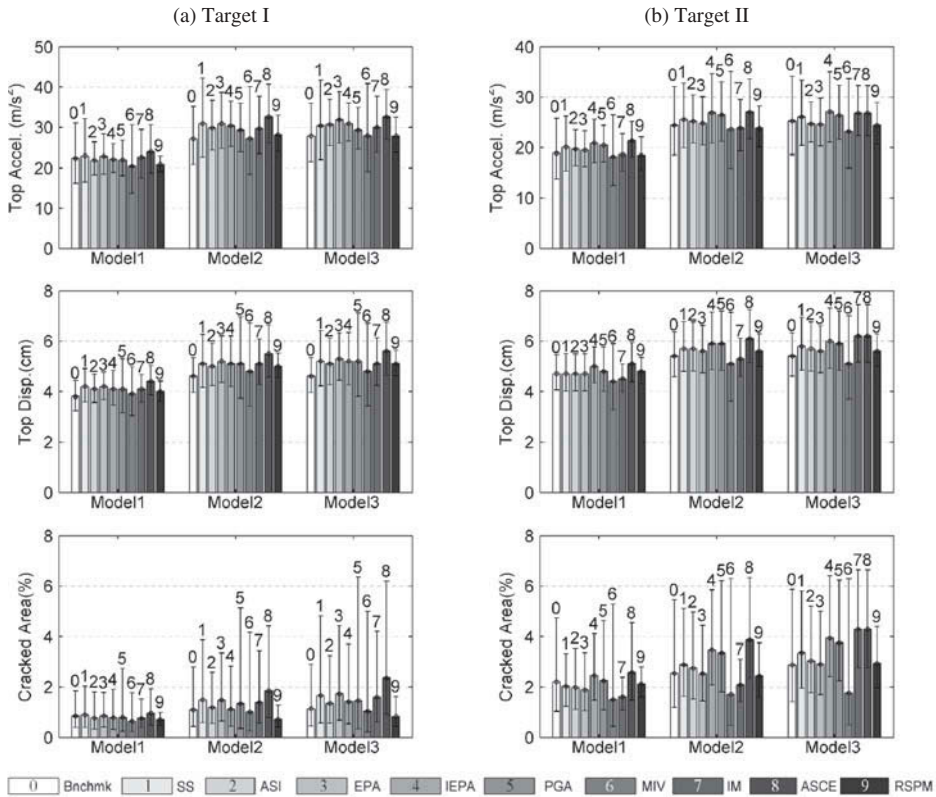


Figure 7. Comparison of the predictions obtained with different scaling methods for different EDPs.

increase in the dispersion was just as possible for different scaled sets. The dispersion was always reduced by the sets scaled with spectral matching; however, the mean prediction was substantially lower than the benchmark. Among the other scaling techniques, scaling to the ASI, EPA, and IEPA appeared to yield a meaningful, if small, reduction in the dispersion compared with the benchmark results. MIV and PGA scaling, on the other hand, led to significant increases in the dispersion for the damage-level EDP on the systems.

4.3. Investigation of the Required Number of Records

The number of motions that can be used to predict the mean response reasonably well is often a very important question in a design process. From the geophysical perspective, an increased number of motions may help with the inclusion of expected phenomena at a design site, while from the engineer’s perspective, it directly determines the computational load. The ASCE/SEI-7-10 [ASCE, 2010] provides the well-known and commonly used suggestions to this end. If three different ground motions are used for the seismic assessment of a structural system, the maximum of the response quantities from each different motion

can be used as a design quantity. Including seven or more ground motions in a study, the designer can use the mean value of the EDPs from these analyses as the response quantity.

Considering the sizes and the associated computational load with the nonlinear dynamic analyses, engineers would want to work with as small a ground motion set as possible. However, the reduction of the number of motions in a ground motion set is strongly dependent on the particular scaling technique's efficiency for reducing the variance in the desired EDP. In order to study this effectiveness, the ability of the chosen sets to adequately predict the benchmark mean was investigated. For the complete sample of sets that could be formed using "n" number of motions out of the 15 original, the sample statistics of the mean were compiled. "Adequate" prediction was chosen in line with the design process, i.e. the percentage of the sample results outside an acceptable bound around the mean was calculated. Prediction of a (mean) EDP lower than 90% and higher than 150% of the benchmark mean was assumed as unacceptable. Obtained henceforth, the percentage of the unacceptable ground motion sets for each scaling procedure is presented for the cracked area ratio EDP in Fig. 8. The large variance in the prediction of this EDP, even after the scaling of the ground motions, is clearly observed. For the first model and the first target spectrum, ASCE, SS, and EPA methods were the most effective scaling techniques. For the second target spectrum, ASCE, IEPA, and RSPM scaling were effective. For models 2 and 3, the effective methods were obtained differently. ASI scaling appears to be the most effective technique for models 2 and 3 at the first target spectrum. The stripe scaling (SS) was more effective for the second target spectrum although scaling to the ASI was almost as successful. Scaling to the IEPA can also be considered reasonably effective for both spectra for these models.

The number of motions required to predict the benchmark result was significantly reduced when the crest displacement was selected as the EDP (Fig. 9). Except for the MIV scaling, all scaling techniques performed well. Use of three GMTHs was adequate for predicting the benchmark displacement mean effectively. Such a satisfactory prediction of the displacement EDP by the methods, and the corresponding discrepancy with the number of motions required for predicting the damage level on the system showed that

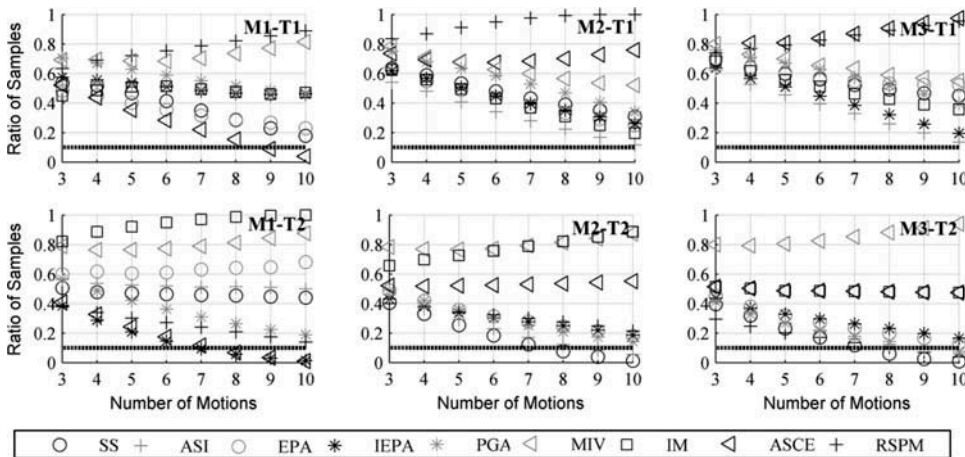


Figure 8. Probability of the mean cracked area ratio of the sample set \leq Benchmark Mean $\times 0.9$ or \geq Benchmark Mean $\times 1.5$.

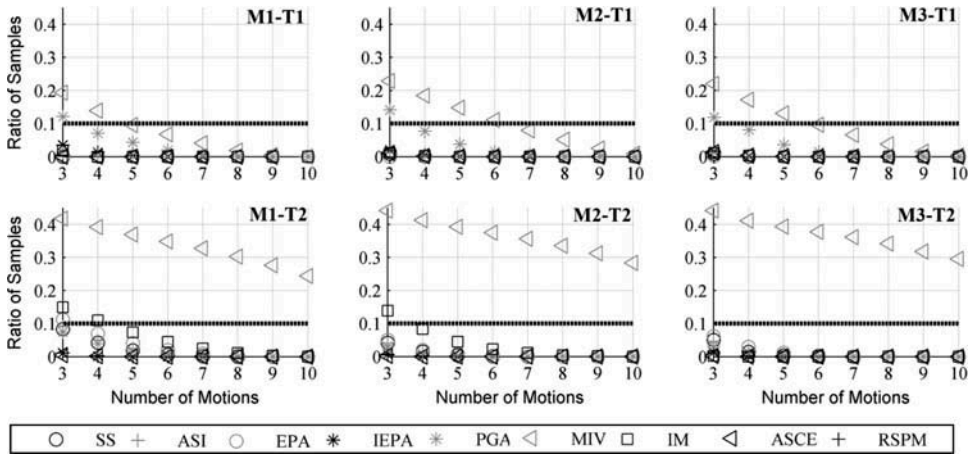


Figure 9. Probability of the mean crest displacement of the sample set \leq Benchmark Mean $\times 0.9$ or \geq Benchmark Mean $\times 1.5$.

the crest displacement was a poor indicator for quantifying the performance level of these systems, in contrast to the typical use of displacement quantities for the damage-level assessment of moment frames.

In conclusion, for predicting the performance of these low-period, brittle structures, scaling to the IEPA and ASI values stands out among the various choices as the most effective procedures working for the majority of the cases considered. The number of motions for a GMTH suite was obtained differently for the two target spectra: results for the first target spectrum displayed a need for the use of 9–10 motions to be included in a given set, while the corresponding number was somewhat lower for the second.

5. Summary and Conclusions

In this study, the use of different ground motion scaling methods for the seismic assessment of concrete gravity dams was investigated from the perspective of accuracy and efficiency in the prediction of the performance levels of the systems. Target spectrum for two alternative sites was determined from the corresponding PSHA. Benchmark solutions were obtained by forming ground motion bins for these two sites. Comparison sets were formed from different records and scaled for use in nonlinear transient analysis of a range of gravity dam models. The models were investigated for the crack patterns occurring on the structures as well as the crest displacement and acceleration. The following conclusions can be drawn based on the results of this study.

- The effect of ground motion direction, insignificant for crest displacement, was substantial for determining the damage level on the system.
- The crest acceleration and the normalized displacement at the crest were relatively accurately predicted by the scaled set within 10% of the benchmark, almost regardless of the technique. In other words, the mean values from the scaled sets were reasonably near the mean levels for the benchmark set with the un-scaled motions. However, significant discrepancy between the benchmark mean and the damage

level predicted using the scaled set was observed for some of the scaling techniques. The worst predictions on the lower and higher sides of the benchmark were obtained by the RSPM and ASCE scaling, respectively. The deviation with respect to the benchmark mean was varying for the other scaling techniques.

- For predicting the performance of concrete gravity dam monoliths, scaling to the IEPA and ASI values stands out among the various choices as the most effective procedures working for the majority of the cases considered.
- The required number of ground motions for an effective prediction of the damage level was obtained considerably higher than the seven motions commonly suggested for this goal. Motion suites comprising 9–10 GMTHs should be formed in order to obtain a close or a reasonably conservative estimate to the design goal.

The results of the study show that the scaling techniques commonly used for the design and assessment of moment frame structures should not be readily applied to the dam structures with the purpose of a performance-based assessment similar to buildings.

Funding

This study was conducted with the funding provided by The Scientific and Technological Research Council of Turkey (TUBITAK) under the grant 5130011.

References

- Aldemir, A., Binici, B., Arici, Y., Kurc, O. and Canbay, E. [2015] “Pseudo-dynamic testing of a concrete gravity dam,” *Earthquake Engineering and Structural Dynamics* **44**, 1747–1763. DOI:10.1002/eqe.2553.
- Alembagheri, M. and Ghaemian, M. [2012] “Seismic assessment of concrete gravity dams using capacity estimation and damage indexes,” *Earthquake Engineering and Structural Dynamics* **42**, 123–144.
- American Society of Civil Engineers [ASCE]. [2010] *ASCE/SEI-7-10 Minimum Design Loads for Buildings*, American Society of Civil Engineers, Reston, VA.
- Applied Technology Council [ATC]. [1978] *Tentative Provisions for the Development of Seismic Regulations for Buildings*, Publication ATC-3-06, Washington, D.C.
- Ay, B. Ö. and Akkar, S. [2012] “A procedure on ground motion selection and scaling for nonlinear response of simple structural systems,” *Earthquake Engineering and Structural Dynamics* **41**, 1693–1707.
- Ay, B. Ö., Fox, M. J., and Sullivan, T. J. [2017] “Technical note: Practical challenges facing the selection of conditional spectrum-compatible accelerograms,” *Journal of Earthquake Engineering* **21**(1), 169–180.
- Baker, J. W. [2011] “Conditional mean spectrum: Tool for ground-motion selection”, *Journal of Structural Engineering* **137**(3), 322–331.
- Bernier, C., Monteiro, R., and Paultre, P. [2016] “Using the conditional spectrum method for improved fragility assessment of concrete gravity dams in Eastern Canada”, *Earthquake Spectra* **32**(3), 1449–1468.
- Bhattacharjee, S. S. and Leger, P. [1994] “Application of NLFM models to predict cracking in concrete gravity dams,” *Journal of Structural Engineering* **120**, 1255–1271.
- Bommer, J. J. and Acevedo, A. B. [2004] “The use of real earthquake accelerograms as input to dynamic analysis,” *Journal of Earthquake Engineering* **8**, 43–91.

- Calayir, Y. and Karaton, M. [2005] "Seismic fracture analysis of concrete gravity dams including dam-reservoir interaction," *Computers and Structures* **83**, 1595–1606.
- Chopra, A. K. and Chakrabarti, P. [1973] "The Koyna Earthquake and the damage to Koyna Dam," *Bulletin of the Seismological Society of America* **63**, 381–397.
- Fenves, G. and Chopra, A.K. [1984] *EAGD-84: A Computer Program for Earthquake Response Analysis of Concrete Gravity Dams*, Earthquake Engineering Research Center Report No. EERC-84/11, University of California, Berkeley, CA.
- Ghaemian, M. and Ghobarah, A. [1999] "Nonlinear seismic response of concrete gravity dams with dam: Reservoir interaction," *Engineering Structures* **21**, 306–315.
- Hancock J., Watson-Lamprey J., Abrahamson N. A., Bommer J. J., Markatis A., McCoy E., Mendis R. [2006] "An improved method of matching response spectra of recorded earthquake ground motion using wavelets," *Journal of Earthquake Engineering* **10**, 67–89.
- Hariri-Ardebili, M. A. [2014] "Impact of foundation nonlinearity on the crack propagation of high concrete dams," *Soil Mechanics and Foundation Engineering* **51**, 72–82.
- Hariri-Ardebili, M. A., Seyed-Kolbadi, S. M., and Kianoush, M. R. [2016] "FEM-based parametric analysis of a typical gravity dam considering input excitation mechanism," *Soil Dynamics and Earthquake Engineering* **84**, 22–43.
- Haselton, C. B. [2009] "Evaluation of ground motion selection and modification methods: Predicting median interstory drift response of buildings," PEER Report 2009/01.
- Jalayer, F., Franchin, P. and Pinto, P.E., [2007]. "A scalar damage measure for seismic reliability analysis of RC frames", *Earthquake Engineering and Structural Dynamics*, **36**(13), 2059–2079.
- Jayaram, N., Lin, T., and Baker, J. W. [2011] "A computationally efficient ground-motion selection algorithm for matching a target response spectrum mean and variance," *Earthquake Spectra* **27**, 797–815.
- Kalkan, E. and Chopra, A. [2010] "Practical Guidelines to Select and Scale Earthquake Records for Nonlinear Response History Analysis of Structures," US Geological Survey Open-File Report, 1068.2010: 126.
- Kalkan, E. and Chopra, A. K. [2011] "Modal-pushover based ground motion scaling procedure," *Journal of Structural Engineering* **137**, 298–310.
- Kramer, S. L. [1996] *Geotechnical Earthquake Engineering*, Prentice Hall, Upper Saddle River, NJ, USA, 653 pp.
- Kurama, Y. and Farrow, K. [2003] "Ground motion scaling methods for different site conditions and structure characteristics," *Earthquake Engineering and Structural Dynamics* **32**, 2425–2450.
- Lysmer, J. and Kuhlemeyer, R. L. [1969] "Finite dynamic model for infinite media," *Journal of the Engineering Mechanics Division*, Proc. ASCE **95**, 859–876.
- Mirzabozorg, H. and Ghaemian, M. [2005] "Nonlinear behavior of mass concrete in three-dimensional problems using a smeared crack approach," *Earthquake Engineering & Structural Dynamics* **34**, 247–269.
- O'Donnell, A., Kurama, Y., Kalkan, E. and Taflanidis, A. [2013] "Experimental evaluation of ground motion scaling methods for nonlinear analysis of structural systems," ASCE Structures Congress, Bridging Your Passion with Your Profession pp. 2180–2191.
- PEER. [2016] Strong motion database [30 November 2016].
- Rots, J. G. [1988] "Computational modeling of concrete fracture," Ph.D. Dissertation, Delft University of Technology, Delft.
- SeismoSoft. [2013] SeismoMatch-A computer program for spectrum matching of earthquake records, available from url: www.seismosoft.com.
- Soysal, B. F., Binici, B. and Arici, Y. [2016] "Investigation of the relationship of seismic intensity measures and the accumulation of damage on concrete gravity dams using incremental dynamic analysis," *Earthquake Engineering and Structural Dynamics* **45**, 719–737. DOI: [10.1002/eqe.2681](https://doi.org/10.1002/eqe.2681).
- Stewart, J. P., Chiou, S.-J., Bray, J. D., Graves, R. W., Somerville, P. G. and Abrahamson, N. A. [2001] "Ground motion evaluation procedures for performance-based design", PEER Report 2001/09, Pacific Earthquake Engineering Research Center, University of California, Berkeley.

- Tinawi, R., Leger, P., Leclerc, M. and Cipolla, G. [2000] “Seismic safety of gravity dams: from shake table experiments to numerical analysis,” *Journal of Structural Engineering* **126**, 518–529.
- TNO DIANA. [2014] User’s manual, R. 9.6.
- United States Army Corps of Engineers [USACE] [2003] “Time-history dynamic analysis of hydraulic concrete structures,” Report No. EP-1110-2-6051, Washington, DC, USA.
- United States Bureau of Reclamation [USBR] [2013] “State-of-practice for the nonlinear analysis of concrete dams at the Bureau of Reclamation,” Denver, CO.
- Von Thun, J., Roehm, L., Scott, G. and Wilson, J., [1988]. “Earthquake ground motions for design and analysis of dams”, *Earthquake Engineering and Soil Dynamics II—Recent Advances in Ground-Motion Evaluation*, Geotechnical Special Publication **20**, 463–481.
- Yakut, A. and Yilmaz, H. [2008] “Correlation of Deformation Demands with Ground Motion Intensity”, *Journal of Structural Engineering*, **134**(12), 1818–1828.
- Yamaguchi, Y., Hall, R., Sasaki, T., Matheu, E., Kanenawa, K., Chudgar, A. and Yule, D. [2004] “Seismic performance evaluation of concrete gravity dams,” 13th World Conference on Earthquake Engineering, Paper no. 1068, Vancouver, B.C., Canada
- Yang, D., Pan, J. and Li, G., [2009]. “Non-structure-specific intensity measure parameters and characteristic period of near-fault ground motions”, *Earthquake Engineering and Structural Dynamics*, **38**(11), 1257–1280.